Cometary globules in the south-east quadrant of the Rosette Nebula

Nimesh A. Patel[1]

Taoling Xie[1,2]

Paul F. Goldsmith[1]

1. Five College Radio Astronomy Observatory

Department of Physics and Astronomy

University of Massachusetts

Amherst, MA 01003

2. Radio/Submm Astronomy Group

MS 160-506"

JPL/Caltech

Pasadena, CA 91109

Received:

Abstract

We present a study of newly identified cometary globules in the south-east quadrant of the Rosette Nebula using the J=1-0 transition of carbon monoxide. The globules are found to be blue-shifted by about 6 $km\ s^{-1}$ with respect to the adjacent Rosette Molecular Cloud. The masses of the globules vary from 50 to 300 $M_{\odot}$, and their sizes are between 1 and 3 pc. Two of the globules have cometary morphology and show velocity gradients of $\sim 1.5\ km\ s^{-1}\ pc^{-1}$ along their symmetry axes. These globules are associated with the IRAS sources 06314+0421, X0632+043, 06322+0427 and 06327+0423 which coincide with local maxima in the ^{13}CO emission. The derived physical parameters of the globules are found to be consistent with those predicted by recent theoretical models of photoevaporating cometary clouds. We suggest that star formation induced by radiation driven implosion has occurred.

1 Introduction

Several recent studies have suggested that radiation driven implosion is a significant mechanism for inducing star-formation in molecular clumps located in the neighborhood of O stars (Klein, Whitaker & Sandford 1985; Sugitani *et al.* 1989; Bertoldi 1989; Bertoldi & McKee 1990; Sugitani, Fukui & Ogura 1991). These clumps presumably evolve from the projections on the surface of a giant molecular cloud, which are typically convoluted (Dickman, Horvath & Margulis 1990; Falgarone, Phillips & Walker 1991). The clumpy structure at the surface of the molecular cloud allows the UV radiation from a neighboring HII region to penetrate deep into the cloud (Stutzki *et al.* 1988; Boissé 1990; Cox, Deharveng & Leene, 1990; Tauber & Goldsmith 1990; Goldsmith *et al.* 1992; Elmegreen 1992),

If sufficiently intense, the UV flux can have a significant influence on the clumps and result in their taking on a cometary shape, with bright rims roughly facing the direction of the exciting star(s). These bright rims were first noticed by Duncan (1920), and were later studied in detail at optical wavelengths (Pottasch 1956; 1958a; 1958b; Osterbrock 1957; Dibai 1960 and Schneider & Elmegreen 1979). An evolutionary sequence based on morphology has been suggested by Reipurth (1983), Leung (1985) and Elmegreen (1992). Sugitani, Fukui & Ogura (1991) have recently published an optical catalog of 44 such objects in the northern hemisphere, which are associated with IRAS point-sources. While these studies reveal the morphological features of the globules and are useful for identifying associated objects, the internal kinematic structure of the globules and their motion with respect to the surrounding interstellar medium, as well as their masses and other properties, can be revealed only by detailed

spectral-line observations at millimeter wavelengths. Radio observations can also reveal newer globules which may be missed by optical studies due to their having insufficient column density or to the presence of excessive diffuse brightness. However, few such studies have been made so far. The elephant-trunk globules in the north-west quadrant of the Rosette Nebula have been studied by Schneps, Ho & Barrett (1980), the cometary globules in IC1396 by Wootten *et al.* (1983), Nakano *et al. (1* 989), Duvert *et al.* (1990) and Serabyn, Gusten & Mundy (1992), and those in the Gum Nebula by Harju *et al.* (1990), Sahu *et al.* (1988) and Sridharan (1992).

A well known example of an H I I region showing the presence of speck and elephant-trunk globules is the Rosette Nebula in Monoceros (NGC 2237-44) which is at a distance of about 1600 pc (Turner 1976). Optical and 4.75 GHz radio continuum emission (Celnick 1985) indicates the presence of ionized gas around the nebula which reaches the boundary of the molecular gas. Cox, Deharveng & Leene (1 990) have studied the IRAS emission from the Rosette Nebula and the surrounding molecular cloud. Recently, Kuchar, Blitz & Bania (1992) have found an expanding H I shell around the Rosette Nebula.

Cometary globules have been recently found in the south-east quadrant of NGC 2244 (Block 1990, Block, Dyson & Madsen 1992; Sugitani, Fukui & Ogura 1991). These globules exist near the Rosette Molecular Complex mapped in ^{12}CO (hereafter CO) and ^{13}CO by Blitz & Thaddeus (1 980) and Blitz & Stark (1986). One of the globules shows the presence of a bright rim that roughly faces the cluster of young stars in the Rosette Nebula. The exciting stars in NGC 2244 are located roughly north-west of this region at a projected distance of $\sim$25 pc.

Although CO emission has been detected from the region covered by these

objects (Blitz & Stark 1986), due to relatively low angular resolution and coarse sampling, the morphology and kinematics of the globules remain unclear. We have surveyed this region with resolution and sampling improved by about a factor of 2 compared to the previous observations. In this paper we report the results obtained from our fully sampled CO and ^{13}CO maps of this region. In the next section we present the observational procedure. In Section 3 we give the results, derive the physical conditions in the globules, and discuss their morphology, kinematics and IRAS association. We compare our observational results with some of the theoretical models of cometary globules in Section 4, and summarize our conclusions in Section 5.

2 Observations

We mapped a 0.5° x 0.5° region in CO and ^{13}CO J= I-O transitions with the the FCRAO 14-m Telescope at New Salem, Massachusetts, during October and November 1991. We used the 15-element QUARRY receiver (Erickson *et al. 1992)* with a set of filterbanks each having 32 channels and a velocity resolution of 0.65 $km\,s^{-1}$ (at 115 GHz) as the primary spectrometer. The typical system temperature (SSB), referred to above the Earth's atmosphere, was about 700K at 115 GHz and about 500K at 110 GHz. The data was acquired in position-switching mode with the reference position at $\alpha(1950) = 06^h37^m43.8^s$, $\delta(1950) = 04°43'08"$ (Blitz and Stark 1986), and calibration was achieved using a chopper-wheel. The pointing and gain calibration were checked by observing SiO maser sources anti planets. The rms pointing error was about 5" and the main beam efficiency was estimated to be $\sim$ 0.45 at both frequencies.

AFGL 961, located at $\alpha(1950) = 06''31'''58'$, $6(1950) = +04"15'30"$ (Blitz

and Thaddeus 1980), is the central position in the CO and ^{13}CO maps. The spacing of the data points is 25" and the half-power beamwidth is about 45" at 115 GHz. At the distance of Rosette, 1' is equivalent to 0.47 pc. The rms noise in each channel is typically 0.2 K in CO and 0.1 K in ^{13}CO.

3 Results

3.1 Morphology and kinematics

Fig. 1 shows the POSS red print of the south-east quadrant of the Rosette Nebula together with a map of integrated ^{13}CO emission. Figs. 2 and 3 show the channel maps of CO and ^{13}CO emission, respectively. The optical emission in Fig. 1 corresponds mostly to the ionizing radiation from the central stars in the Rosette Nebula, and it appears to be anti-correlated with the CO emission. The lack of CO emission from the region around $(\alpha, \delta) = (06^h32^m\ 10', 04022')$ in Fig. 1, or $(\Delta\alpha, \Delta\delta) = (5', 5')$ in Figs. 2 & 3, is presumably due to the dissociation of molecules by UV radiation which has penetrated relatively deeply into the edge of the molecular cloud. The presence of a rich velocity structure in this region is evident from the channel maps, We see that the globules appear in the velocity range between 8 and 12 $km\ s^{-1}$, while the stronger extended emission exists between velocities of 12 and 17 $km\ s^{-1}$. In Fig. 1, the ^{13}CO emission is integrated between 5 $km\ s^{-1}$ and 12 $km\ s^{-1}$. The corresponding map of integrated CO emission appears similar to that shown in Fig. 1, in which the globules are identified and labeled. The stronger extended emission shown in Figs. 2b and 3b corresponds to the region of strongest emission in the Rosette molecular cloud which was mapped by Blitz and Thaddeus (1980). It is clear from Figs. 2a and 2b that the globules are blue-shifted by $6 - 7\ km\ s^{-1}$ with respect to the Rosette cloud. Since objects 1- 6 appear relatively well isolated,

we refer to them as globules. Objects 7-9 (clumps) appear to be superposed over the emission from the Rosette cloud, but they have the same velocity as the globules.

in Fig. 2b, the peak in CO antenna temperature appears at $\sim 15\,km$ S-l at $(\Delta\alpha, \Delta\delta) = (-7', 12')$. Blitz & Thaddeus (1980) found this location to be the peak in CO emission throughout the Mon OB2 complex. This peak coincides with the location of lRAS 06314+0427 (Cox, Deharveng & Leene 1990; Block 1990). We refer to this source hereafter as IRS (note that Blitz and Thaddeus refer to AFGL 961 as 'IRS').

At the location of AFGL 961, Blitz and Thaddeus (1980) fount] CO emission to be self-absorbccl, in a region roughly elongated towards the north-west with an extension of about 1 *pc* x 3 *pc*. From Fig. 2a, at 11 and 11.7 $km\ s^{-1}$, there appears a lack of CO emission in a, narrow region passing through the location of AFGL 961 and inclined towards the north-west; while in Fig. 3a, the ^{13}CO emission appears continuous in this region at these velocities. 'J'bus, wc see that the region over which CO self-absorption occurs is significantly larger than was indicated by Blitz and Thaddeus (1980). When compared to the ^{13}CO emission, the absorption dip in CO line-])rofiles is slightly blue-shifted. Self-reversed profiles arc seen from a few other regions in giant molecular clouds (Snell & Loren 1977; Blitz & Thaddeus 1980; Leung & Brown 1977) and have often been interpreted as an indication of collapse of outer cool gas onto a hotter core. This explanation may not hold for the region around AFGL 961 as the dip is Lluc-shifted and since the area over which the clip occurs is much larger than the typical expected size of a collapsing region. A similar phenomenon has also been noticed by Xic (1 992) in the Mon R2 core.

We now discuss the observed properties of the globules. Globules 1 and

3 clearly have cometary shapes, while globule 2 appears to be a fragmented extension from globule 1. Near the location of globule 6, Block (1990) identified optically three cometary globules all pointing roughly in tile direction of IRS. Possibly due to ham-dilution, these cometary globules do not appear distinctly on our CO maps. However, globule 6 is elongated roughly in the same NW-SE direction as the optical cometary globules. A spatial-velocity cut through this object along this direction shows a velocity gradient of $\sim 0.6\ km\,s^{-1}\,pc^{-1}$.

Globule 1 has been identified optically by Block (1 990) and by Sugitani, Fukui & Ogura (1991) (object number 24 in their catalog). Fig. 4 presents a superposition of the CO, ^{13}CO and optical emission from this object. '1'here is a definite correspondence between the region of visible extinction and the ^{13}CO emission. However, the optical size of the globule is significantly smaller than indicated by molecular tracers. Although CO emission is widespread over the optical image of the globule, extending beyond the tail, the ^{13}CO emission is confined to the head of the globule. Fig. 5 shows a montage of the CO and ^{13}CO spectra in the head region. The ratio of ^{13}CO to CO antenna temperature increases systematically towards the western boundary of the globule's head. This could indicate a gradient in either temperature or column density (or both). However, since this ratio approaches unity, it is more likely to indicate an enhancement in optical depth in this region just inside the bright rim. The antenna temperature of both the species decreases dramatically in this region which is consistent with the photodissociation expected at the rim.

As noted by Block (1990), the symmetry axis of globule 1 seems to point towards IRS. Fig. 6 shows a spatial-velocity CO map cutting through globule 1 in this direction ('a' in Fig. 1). The velocity separation of the globule relative to IRS is about 6 km/s, Within the globule, there is a velocity gradient of about

1.6 km S-l pc 1 We also see a velocity gradient in the opposite direction across the emission associated with IRS of ~ 0.5 km s-' PC-l. A spatial-velocity cut along a north-west direction ('b' in Fig.1) across globules 5,3 and 1 is shown in Fig. 7. The complicated structure of velocity gradients in different globules is apparent in this Figure.

Table 1 summarizes the observed physical properties of the globules. All the globules and clumps appear to be at a V_{LSR} of ~ 9 km s^{-1}. 'J'heir sizes vary from 1 to 3 pc; globule 6, however, is the most elongated having a length of about 5 pc. Assuming CO emission to be optically thick and ^{13}CO to be optically thin, and assuming LTE, wc calculate column densities and kinetic temperatures towards the central regions of the globules according to the method of Dickman (1978). The kinetic temperatures T_k listed in Table 1 are estimated from the CO antenna temperature, assuming a beam-filling factor of 1. The column densities listed in Table 1 are the mean values in the central regions of the globules, and vary from 1---7 x 10^{21} cm^{-2}. The masses were calculated from the LTE column density in each pixel. With the usual uncertainties associated with the LTE method, the globule masses may be in error by about a factor of 2 (not including the uncertainty in the distance to the Rosette Nebula). Additional uncertainty is present for clumps '7 and 8 due to confusion with emission from IRS.

3.2 IRAS associations

As noted by Cox, Deharveng &Leene990), many of the molecular clumps in the Rosette region arc associated with IRAS sources. Table 2 lists the IRAS sources associated with the objects we have identified. The far infrared luminosities appearing in Table 2 were calculated using the following formula (Casoli

et al. 1986),

$$L_{IR} = 4.7 \times 10^{-6} D^2 \left(\frac{S_{12}}{0.79} + \frac{S_{25}}{2} + \frac{S_{60}}{3.9} + \frac{S_{100}}{9.9} \right) L_{\odot} \qquad (1)$$

where D is the distance in pc and S_λ is the flux density in Jy. In globule 1, IRAS 06322+0427 appears faintly on the POSS red print, at the location of the peak in ^{13}CO emission (sew Fig. 4). This source is located at a distance of about 0.5 pc behind the rim. Within the sensitivity of our observations (sew Fig. 5), the spectra do not show any indication of an outflow near this IRAS source. Wc have also detected CS J=2- 1 emission from the location of this IRAS source where it appears to have a peak. This spectrum is shown in Fig. 8. Following Goldsmith *et al.* (1992), and assuming a value of 10-B for the abundance of CS relative to H_2, wc estimate a density of $\sim$8 x 103 $c\,m^{-3}$ (averaged over the beam), at this location.

Two IRAS sources arc found to bc associated with globulc 3. Of these, X0632+043 is from the IRAS Small Scale Structure Catalog, and has a relatively large positional uncertainty ($\sim$ 4'). Fig. 9 is a plot of integrated ^{13}CO emission from globulc 3 which shows two peaks in emission separated by $\sim$ 1.5 *pc* along cmt-west. IRAS 06314+0421 also appears near the peak in ^{13}CO t-mission in globulc 7. All these 1 RAS point sources have colors which arc characteristic of those sources associated with dense cores (Emerson 1987; Parker 1991) and it thus seems plausible that these infrared sources arc embedded within the globules.

4 Discussion

Our CO ond ^{13}CO mapping has revealed the following distinguishing characteristics of the globules in the SE quadrant of the Rosette Nebula: (1) they

appear cometary in shape (Figs. 1,4 & 9); (2) their velocities are blue-shifted with respect to the Rosette Molecular Cloud by about $6\,km\,s^{-1}$ (Figs. 2 &3); (3) they have internal velocity gradients (Figs. 6 & 7) and (4) they show signs of star formation as suggested by the presence of IRAS point sources at the location of peaks in ^{13}CO emission (Figs. 4 & 9). Globule 1 also shows the presence of a bright rim roughly facing NW (Figs. 1 & 4) towards the exciting stars of the NGC 2244 HII region, We now briefly discuss in the context of our observations some of the theoretical models, which arc relevant to understanding the structure and origin of these cometary globules.

An early idea suggests that cometary globules evolve from elongated protrusions (elephant trunk globules) which are caused by Rayleigh-Taylor instability in a shell of dense gas which is external to and pressurized by hot ionized gas (Pottasch 1958b, Herbig 1974). As shown by Schneps, Ho & Barrett (1980), the elephant trunk globules in the NW quadrant of the Rosette Nebula were most likely created by a Rayleigh-Taylor instability. The SE globules discussed here differ in a number of respects from those in the NW quadrant. The SE globules appear to be farther away from the central exciting source of the HII region, while the NW globules project into the H II region from the interface between the HII region and the molecular material, The SE globules lie in a relatively quiescent region and are visible only on enhanced 1'0SS images, while the NW globules appear as silhouettes against the bright $H\alpha$ emission from the 1111 region. The globulin evolved from the elephant trunks in the NW are typically very small (0.02-0.2 pc), and arc referred to as tear-drop globules (Herbig 1974, Cernicharo 1991). The sizes of the SE globules arc, on the other hand, typically larger than 1 pc (Table 1 .). If the SE globules were created by Rayleigh-Taylor mechanism, the observed internal velocity gradients should be due to the stretching of the

globule, as discussed by Schneps, Ho and Barrett, then the velocity gradients should occur along directions nearly parallel to each other, which is not what is observed (see Figs. 6 & 7). In this scenario, cometary globules are the tips of the inward-projecting tongues of material. As such, they should have a smaller outward velocity (relative to central star of HII region) than the material of the shell at their base. In fact, we see the SE globules in projection against the HII region, but they are blue-shifted compared to the extended emission, opposite from what would be expected in this picture. Hence, we feel that the Rayleigh-Taylor mechanism is less likely to be the cause for the globules in the SE quadrant of Rosette Nebula.

Another possibility is that the SE globules have formed from fragmentation of an unstable layer between the ionization front and the shock front at the interface between the neutral and the ionized region (Elmegreen & Lada 1977). If we assume a density of $10^3\ cm^{-3}$ for the molecular cloud, a temperature of 100 K for the cooled, postshock (CPS) layer, and an O star column density of 10 per $100\ pc^2$, we obtain from Eq. 13 of Elmegreen & Lada (1977) that the thickness of the CPS layer would be $\sim 0.6\ pc$ at a distance of 25 pc from the central exciting source. This value is considerably smaller than the size of the region occupied by the globules. One may argue that the CPS layer which was fragmented and led to the formation of the globules is almost normal to the line of sight. However, the apparent cometary form of the globules suggests otherwise. The velocity of the shock given by Eq. 7 of Elmegreen & Lada, for a distance of 25 pc, is $4.2\ km\ s^{-1}$. This is comparable to the velocity of the globules with respect to the Rosette Molecular Complex. According to Elmegreen & Lada, due to the inhomogeneities in the molecular cloud, different parts of the shock will be at different distances from the exciting star with a resulting difference in velocity

given by $\Delta v_s/v_s \sim \Delta r/4r$. Using the observed value of the velocity of globules for $v_s \sim 6\,km$ S-*, and a typical separation of ~ 5 pt., we get $\Delta v_s \sim 0.05\ km$ s-l, which is considerably smaller than the observed velocity spread of $\sim 0.25\ km\,s^{-1}$ as seen from "1'able 1. With these considerations, while wc cannot completely rule out the possibility that the globules have resulted from a CPS layer, the Elmegreen & Lada mechanism is not highly compelling.

An intense flux of UV radiation can cause the implosion of a neutral cloud as studied numerically by Sandford, Whitakcr & Klein (1 982) and by Klein, Whitakcr & Sandford (1985). A detailed analytical study of photoevaporating globules has been made by Bertoldi (1989) and Bertoldi & McKee (1990), who also demonstrated the consistency of their theory with the observed parameters of the elephant-trunk globules in the north-west quadrant of the Rosette Nebula and the cometary globules in the Gum Nebula. An application of this theory has also been rnadc recently to an observational study of a bright rim in NGC 2264 by Tauber, Lis & Goldsmith (1992), who found it to be reasonably consistent with their observations. in the formalism of Bertoldi & McKee (1990), a cloud surviving the UV radiation will settle into an equilibrium cometary configuration in a sound crossing time, while accelerating away from the exciting source. Thus this model appears of considerable interest for understanding the SE globules.

Given that molecular clouds arc typically very clumpy (Stutzki *et al. 1988;* Boissé 1990; Tauber & Goldsmith 1990; Elmegreen 1992), wc prefer the interpretation that the cometary globules have evolved from pre-existing clumps in the molecular cloud, under the effect of UV radiation from the central OB stars in NGC 2244. Due to clumpiness in the molecular cloud, the ionizing radiation penetrates into the cloud effectively, and reaches the dense clumps in the more distant part of the molecular cloud. The initial conditions in the clumps favor

a]1-type ionization front which drives a shock inside the clumps which evolve to become globules. These globules subsequently maintain a stationary state in which they appear to have a cometary form. Since the globules appear as enhanced extinction in the optical image, and as their velocities are blue-shifted with respect to that of the exciting stars, they arc in the foreground and have been accelerated towards us, away from the Rosette molecular cloud. It is likely that globule 2 is a clump that has fragmented from globule 1 duc to the radiative implosion. A similar phenomenon is also suggested from the ^{13}CO map of the integrated intensity between 9 and 12 $km\,s^{-1}$ in globule 3 as shown in Fig. 9. The IRAS sources 06327+0423 and X0632+043 in globule 3 indicate the possibility of multiple star-formation along the symmetry-axis of a radiatively imploded globule. In the CO observations of the prominent cometary globule in IC 1396, we can see a similar fragmentation along the symmetry axis (see Fig. 3a of Nakano *et al.* 1989).

The influence of the radiation from NGC 2244 is directly indicated by the presence of the bright rim in globule 1. Another indication of this interaction" is seen in a small region that projects out of clump 9 towards the north-east. On the CO spatial-velocity map shown in Fig. 6, this region appears at AS $\approx$ 20', and the size of this projection is $\sim$1 pc. The spectra around this position arc shown in Fig. 10. Wc scc that the narrow red-shifted CO emission (FWHM$\sim$ 1.8 $km\,s^{-1}$, at $V_{LSR} \sim$ ***16*** $km\,s^{-1}$) occurs in the same region that shows the broad blue-shifted emission (FWHM$\sim$ 3 km s-', at VLSR $\sim$ 8.5 km s-'). The ^{13}CO emission is below the sensitivity of our observations. Onc possibility is that this clump has been shocked and the post-shock heated gas is responsible for the broad blue-shifted line while the prc-shocked cooler gas produces the narrower red-shifted (or at ambient velocity) emission (a similar example of

such a phenomenon has been noted earlier by Wilking *et al.* 1$S4 in W5).

Bertoldi (1989) has presented an initial cloud parameter space in terms of cloud column density and a parameter that characterizes the ionization strength. With the source of UV radiation as the central OB stars of NGC 2244 for which the Lyman continuum photon luminosity is $5.8 \times 10^{49}\ photons\ s^{-1}$ (Cox, Deharveng & Leene 1 990), and assuming that our measured mean value of column density is representative of the initial value we find that globule 1 lies in region II of Bertoldi's plot of initial cloud parameter space (see Fig. 1 of Bertoldi 1989). This region corresponds to clouds which will be compressed by an ionization-front-driven shock, with an ionized gas boundary layer (recombination layer) that is thin compared to the size of the globule. Clouds of these characteristics will be accelerated away from the source of the UV radiation rather than being completely ionized, as would occur, for example, for lower mass objects.

Based on the optical morphology of the globules, Block (1990) has suggested that they arc largely influenced by stellar-winds from a hidden O7 star at the location of IRS. Due to a smaller distance between the globules and this hidden exciting source at IRS, a smaller value of its luminosity corresponding to a single *07* star, $\sim 0.2\ x\ 10^{49}\ photons\ s^{-1}$, may still produce a flux comparable to that due to the stars in NGC 2244 assuming that the true and projected distances are not very different. However, the spectral type of this hidden object was inferred from the observed far infrared flux assuming a single source of radiation. Subsequent infrared imaging has revealed the presence of a cluster of objects at this location (Block, Dyson & Madsen 1992). This would lead to a smaller value of luminosity for this hidden source. It seems more likely that the globules arc primarily affected by the radiation from NGC 2244 and only weakly influenced by the young stellar object(s) at IRS. The clump associated with this object

(where the CO emission peaks) also lies in region II of Bertoldi's phase diagram. This supports the possibility that IRS may also be a result of radiative implosion as suggested earlier by Blitz and Thaddeus (1980).

From Eq. 3.23 of Bertoldi & McKee (1990), we estimate the pressure due to the hot ionized gas produced by the UV radiation to be 4.1 x $10^{-10} dynes\ cm^{-2}$, assuming the exciting source to be the stars in NGC 2244. We estimate the internal pressure in the globules from their observed linewidths, and find it to be of the order of 1 $0^{-10} dynes\ cm^{-2}$, showing that the globules are likely to be in near pressure equilibrium. The external pressure near the tail region of the globules is expected to be less, and correspondingly these regions in the globules appear more diffuse as seen in Figs. 4 & 9. Block (1990) has suggested that the globules are influenced by a stellar wind from a hidden 07 star at the location of IRS. Eq. 3.36 of Bertoldi and McKee (1 990) gives the ratio of the pressure due to the hot ionized gas to the ram pressure due to the stellar wind from the exciting source. With the exciting source to be the stars in NGC 2244, we find this ratio to be of the order of 3000, while with the exciting source to be a hidden 07 star at the location of IRS, we find this ratio to be shout 200. It appears that the stellar wind would have to be unusually strong in order for it to dominate the effect of the UV radiation. However, as seen from Figs. 1 & 6, the symmetry axis of globule 1 and the direction of the velocity gradient point towards IRS, suggesting an interaction with the source at this location, but the nature of this interaction remains unclear. Further infra-red observations would be helpful to clarify the characteristics of this hidden source.

It is interesting to compare the estimated LTE mass with the virial mass to approximately check if the globules are gravitationally self-bound. Using a value of 0.5 pc for its radius and a ^{13}CO line-width of 1.5 $km\ s^{-1}$ we find the

virial mass of globule 1 to be $\sim 140\ M_{\odot}$, where we have neglected magnetic field and external pressure, and assumed a variation in density as $1/r^2$ (McLaren, Richardson & Wolfendale 1988). For the case of constant density and a density variation as $1/r$, we get 236 and 214 $M_{\odot}$, respectively. These virial mass estimates are greater than or comparable to the 100 $M_{\odot}$ LTE mass of the globule, suggesting that the globule is at best critically self-bound excluding the effect of the radiative implosion. However, the presence of the IRAS source in the head of the globule suggests that collapse has taken place, and thus radiative implosion is likely to have played an important role in star-formation in this globule.

The SE globules are observed to have velocities typically $6\ km\ s^{-1}$ blue-shifted relative to the extended emission in the Rosette molecular cloud. The estimated UV flux at globule 1 and its mass from the CO observations, locates it in the equilibrium cometary cloud mass-flux parameter space defined by Bertoldi & McKee (1990) (see their Figs. 13 & 14), in a region which corresponds to the following characteristics: (1) the globule will not be instantly ionized by the radiation; (2) during its initial radiation driven implosion, it will gain a velocity of $\sim 2{,}5\ km\ s^{-1}$ (Eq. 2.5 of Bertoldi 1989); (3) the globule will move far from its initial position while evaporating. Whether this initial velocity increases to a value close to that observed is difficult to ascertain given the uncertainties in the initial conditions. However, it seems plausible that this mechanism described by Bertoldi & McKee can explain the observed velocities of the SE globules.

The dynamical age of the Rosette Nebula is about $2 - 6 \times 10^5 yr$ (Mathews 1967). NGC 2244 has two stars with spectral types earlier than O6 which have upper age limits of $3 \times 10^6 yr$ (Stothers 1972). The dynamical age inferred from the velocity gradient in globule 1 is $\sim 6 \times 105\ yr$ (see Fig. 6). From the velocity gradients in the elephant-trunk globules in the north-west quadrant,

Schneps, Ho & Barrett (1980) have estimated their age to be $3 - 5 \times 10^5 yr$. We have assumed that the SE globules have evolved from ~lrc-existing clumps under the influence of UV radiation from NGC 2244. We estimate the typical sound crossing time in these clumps to be of the order of $10^7 yr$, neglecting magnetic fields and using a size of 1pc. Using Eq. 4.10a of Bertoldi & McKee (1 990), we find the characteristic evaporation time for globule 1 to be $\sim 4.5 \times 10^7 yr$, somewhat greater than the sound crossing time. However, as noted by Bertoldi aud McKee, if the clump is magnetic (with a typical field strength of the order of $30 \mu G$) then the sound crossing time (Eq. 4.8 of Bertoldi and McKee) is 3.4 x 105yr, significantly less than the evaporation time. Hence a magnetic post-implosion clump would have enough time to settle into an equilibrium cometary configuration as described by the formalism of Bertoldi and McKee, within a time scale that is consistent with the dynamical time scale of the Rosette Nebula and the age of the O type stars noted above. Such cometary globules would then also have the consequences of radiative implosion and acceleration away from the source of UV as described by Bertoldi and McKee, with a typical velocity of about 5 $km\ s^{-1}$. While a more exact confirmation of the calculations of Bertoldi and McKee (1 990) requires further observations, in particular observations of the ionized gas near the bright rim of the globules and observations at higher angular resolution to study the density profiles of the globules, all the major observational features of the globules reported here appear consistent with this model,

5 Summary

Our study of CO and ^{13}CO emission from the newly identified cometary globules in the south-east quadrant of the Rosette Nebula has led to the following main results. The globules are kinematically distinct from the Rosette molecular cloud, having a velocity of $6 - 7$ km s-1 relative to the stars and ionized gas of the 1111 region. Two of these globules appear to be examples of star-formation by radiatively driven implosion of molecular clouds and they provide an opportunity to check the theoretically predicted characteristics of clouds influenced by neighboring young stars. These globules appear to have imploded under the influence of ionizing radiation from the OB stars in NGC 2244. A hidden young stellar object at the position of the CO peak may also be affecting the globules as suggested by their orientation and the directions of internal velocity gradients. However, the central stars in NGC 2244 seem to have had a more significant effect on the globules.

We thank Ron Snell and Frank Bertoldi for helpful discussions, and Chris Salter for suggestions on improving the manuscript. We are grateful to K. Sugitani for providing us the optical photograph of the Rosette region. The Five College Radio Astronomy Observatory is operated with the permission of the The Metropolitan District Commission. This work was supported in part by NSF Grant AST91 15721. This is contribution 791 of the Five College Astronomy Department.

References

Bertoldi, F. 1989, ApJ,346,735

Bertoldi, F., & McKee, C. F. 1990, ApJ,354,529

Blitz, L., & Stark, A. 1986, Ap JL,300,L89

Blitz, L., & Thaddeus, P. 1980, ApJ,24 1,676

Block, D. 1990, Nature,347,452

Block, D., Dyson, J. E., & Madsen, C. 1992, ApJL,390,L13

Boissé, P. 1990, AA,228,483

Casoli, F., Dupraz, C., Gerin, M., Combes, F'., & Boulanger, F. 1986, AA,169,281

Celnick, W. E. 1985, Astron. Astrophys. Suppl.,53,403

Cernicharo, J. 1991, in The Physics of Star Formation and Early Stellar Evolution, Ed: Lada, C. J., & Kylafis, N. D. (Kluwer: Dordrecht), p287

Cox, P., Deharveng, L., & Leene, A. 1990, AA,230,181

Dibai, E. A. 1960, Soviet Astr. J.,4,13

Dickman, R. 1,.1978, ApJS,37,407

Dickman, R. I,., Horvath, M. A., & Margulis, M. 1990, ApJ,365,586

Duncan, J. C. 1920, ApJ,51,4

Duvert, G., Cernicharo, J., Bachiller, R., & Gomcz-Gonzalez J. 1990, AA,233,190

Elmegreen, B. G., & Lada, C. J. 1977, ApJ,214,725

Elmegreen, B. G. 1992, in III Canary Islands Winter School (Cambridge University Press)

Emerson, J. 1'. 1987, in Star Forming Regions, Proc. lAU Symp. No. 115, Ed: Peimbert, M. & Jugaku, J., (Reidel, Dordrecht), p 19

Erickson, N. R., Goldsmith, P. F., Novak, G., Grosslein, R. M., Viscuso, P. J., Erickson, R. B., & Predmore, C. R. 1992 IEEE Trans. on Microwave Theory and Techniques,40,1

Falgarone, E., Phillips, T. G., & Walker, C. K. 1991 ApJ,378,186

Goldsmith, 1'. F., Margulis, M., Snell, R. L., & Fukui, Y. 1992, ApJ,385,522

Goldsmith, P. F., Lis, D. C., lester, D. F., & Harvey, P. M. 1992 ApJ,389,338

Harju, J., Sahu, M., Henkel, C., Wilson, T. 1,., Sahu, K. C., & Pottasch, S. R. 1990 AA,233,197

Herbig, G. 11.1974, PASP,86,604

Klein, R. I., Whitaker, R. W., & Sandford, M. '1'., 1985 in Protostars and Planets II, Ed: D. Black and M. Matthews (Tucson: University of Arizona Press), p 340

Kuchar, '1'., Blitz, L., & Bania, '1'. M. 1992, in preparation

Leung, C. M. 1985, in Protostars and Planets 11, Eel. D. Black and M. Matthews (Tucson: University of Arizona Press), p 104

Leung, C. M., & Brown, R. 1..1977, ApJ,214,L73

McLaren, 1., Richardson, K., M., & Wolfendale, A., W. 1988, ApJ,333,821

Mathews, W. G.1967, ApJ,147,965

Nakano, M., Tomita, Y., Ohtani, H., Ogura, K., & Sofue, Y. 1989, Publ. Astron. Sot. Japan, 41,1073

Osterbrock, D. E. 1957, ApJ,125,622

Parker, N. D.1991, MNRAS,251,63

Pottasch, S. 1956, Bulletin of the Astron. Inst. of the Netherlands,13,77

Pottasch, S. 1958a, Bulletin of the Astron. inst. of the Netherlands,14,29

Pottasch, S. 1958b, Reviews of Modern Physics,30,1053

Reipurth, 11.1983, AA,17,183

Sahu, M., Pottasch, S. R., Sahu, K, C., Wesselius, P. R., & Desai, J. N. 1988, AA,195,269

Sandford, M. T., Whitaker, R. W., & Klein, R. 1.1982, ApJ,260,183

Schneider, S., & Elmegreen, B. 1979, ApJS,41 ,87

Schneps, M. 11., Ho, P. T. 1'., & Barrett, A. 11.1980, ApJ,240,84

Serabyn, E., Gusten, R., & Mundy, L., 1993, ApJ,404,247

Snell, R. L., & Loren, R. 11.1977, ApJ,211 ,122

Sridharan, T. K. 1992, Journal of Astrophysics and Astronomy,1 3,217

Stothers, R. 1972, ApJ,1 75,431

Stutzki, J., Stacey, G. J., Genzel, R., Harris, A. I., Jaffe, D. 'I'., & Lugten, J. B. 1988, ApJ,332,379

Sugitani, K., Fukui, Y., Mizuro, A., & Oshashi N. 1989, ApJ,342,47

Sugitani, K., Fukui, Y., & Ogura, K. 1991, ApJS,77,59

Tauber, J. A., & Goldsmith, 1'. F. 1990, ApJ,356,L63

Tauber, J. A., Lis, D., & Goldsmith, P. F. 1993, ApJ, in press

Turner, D. G. 1976, ApJ,21 0,65

Wilking, B. A., Harvey, P. M., Lada, C. J., Joy, M., & Doering, C. R., 1984, ApJ,279,291

Wootten, A., Sargent, A., Knapp, G., & Huggins, P. J. 1983, ApJ,269,147

Xie, '1'., 1992, Ph. D. Thesis, University of Massachusetts

Figure Captions

Fig. 1 A POSS red print of the Rosette Nebula and surrounding region. The region we m apped, indicated by the rectangle, is expanded in the lower panel showing the integrated ^{13}CO emission in the velocity range 5-12 $km\ s^{-1}$. The contour levels are between 1 and 6 $K\ km\ s^{-1}$, separated by 1 $K\ km\ s^{-1}$. Each grey shaded box represents a sampled spectrum in the map, with the shading scaled linearly with the integrated intensity. The globules we have identified are labeled in this figure. On a large scale, the molecular emission is anti-correlated with the optical brightness which represents ionizing radiation. Globule 3 is not visible in optical extinction, while the three cometary globules detected in the masked photographs by Block (1990) are not evident in CO emission.

Fig. **2a,b** Channel maps of CO emission. The contour levels are separated by 1 K between 2 and 16 K. The globules appear at velocities 8- 12 *km S-l* while the stronger emission from the Rosette cloud appears at 14- 17 *km S-l*. At $(\Delta\alpha, \Delta\delta) = (O', O')$, we note the emission from the AFGL 961 outflow with the red-shifted lobe at around 15 $km\ s^{-1}$ and the blue-shifted lobe at around 9 $km\ s^{-1}$; the bipolarity of the outflow is evident even at low velocities. At (7',11 '), the fragmentation of globule 1 is seen clearly at 9 $km\ s^{-1}$.

Fig. **3a,b** Channel maps of ^{13}CO emission. The contour levels are separated by 0.5 K between 0.5 and 6 K.

Fig. 4 Overlay of the optical image of globule 1 with the CO (dashed contours) and ^{13}CO (solid contours) emission. The CO emission is well confined by the bright rim, showing a sharp decrease in emission at the rim. in the head region there is a clear anticorrelation between the optical and the CO emission but near the tail the CO emission is extended. ^{13}CO is confined to the head of the globule where the density is presumably enhanced clue to the ionization-front-driven shock. The embedded IRAS source is also faintly visible in this POSS red print and it is located near the peak of the LTE column density at a distance of about 0,5 pc behind the bright rim on the symmetry-axis.

Fig. 5 Montage of CO (solid curves) and ^{13}CO broken curves) spectra in the IIcad-region of globule 1. The increasing ratio of ^{13}CO to CO peak intensities towards the direction of the apex at $(\Delta\alpha, \Delta\delta) = (3'.5, 12'.5)$, indicates the increase in column density there due to implosion (offsets measured from AFGL 961, $\alpha(1950) = 06^h31^m58^s$, 6(1950) = +04 °15'30"). Near the location of the rim the CO emission decreases sharply, presumably due to photodissociation by the radiation from the HII region which is Ilort]l-west of the globule.

Fig. 6 Spatial-velocity CO map across globule 1 and IRS along the axis indicated as (a) in Fig. 1. The position offset, AS, is measured from $(\alpha, \delta) \approx (06^h32^m50^s$ 04 °28'30"). This figure shows that the globule is blue-shifted by about 7 $km\ s^{-1}$ with respect to IRS. There is a velocity gradient of 1.6 km S-l pc^{-1} along the direction pointing towards IRS.

Fig. 7 Spatial-velocity map across globules 1,3 and 5 along the direction indicated as (b) in Fig. 1, towards the direction of the central stars in NGC 2244. 'l'he position offset, AS, is measured from $(\alpha, \delta) \approx (6^h33^m, 4°14')$. The velocity gradients seen across globules 1 & 3 arc similar, but are of opposite sign from the gradient seen in globule 5.

Fig. 8 CS J=2-1 emission from the location of the IRAS source 06322+0427 at the head of globule 1.

Fig. 9 Association of IRAS sources 06327+0423 (•) and X0632+043 ('(x") with the peaks in ^{13}CO integrated intensity between 9 and 12 $km\ s^{-1}$ in globule 3. X0632+043 is from the IRAS Small Scale Structure Catalog, and has a positional uncertainty of about 4',4. Contour levels are separated by 0.5 $K\ km\ s^{-1}$ between 1 and 3.5 $K\ km\ s^{-1}$.

Fig. 10 CO and ^{13}CO spectra from a region near clump 9, projecting towards the }11 I region. The narrow CO line represents emission from the preshocked gas that is at the velocity of the Rosette C1OUC1 complex while the post-shock heated gas in the clump is responsible for the broad blue-shifted line.

Table 1: Physical properties of globules

Globule	$\alpha(1950)$ $h\ m\ s$	6(19.50) $o\ '\ ''$	T_k (K)	V_{LSR} km/s	$N(H_2)$ x $10^{21} cm^{-2}$	Mass $M_\odot$	a^1 (pc)	b^1 (pc)	IRAS source
1	063218.5	042750	16.3	8.8	6.8	100	1.4	1.8	06322 +0427
2	063228.0	042345	12.3	9.2	1.1	50	0.'7	0.8	
3	063232.0	042224	15.3	9.7	6.6	150	1.8	2.9	06327+0423 X0632+043[2]
4	063231.9	042224	9.3	9.2	1.6	200	1.5	2.7	
5	063248.6	041953	11.6	9.5	2.2	300	2.3	2.5	
6	063240.2	041312	11.2	9.1	3.4	200	2.1	4.6	
7	063140.0	042044	13.5	9.2	22	100	2.1	2.0	06314+0421
8	063133.3	042610	14.7	9.5	11	100	1.9	1.5	
9	063151.7	042635	11.2	9.2	4.6	50	1.5	1.6	

[1] a is the diameter along the minor axis, and b, along the major axis
[2] From IRAS Small Scale Structure Catalog

Table 2: IRAS sources associated with the globules

IRAS	$\alpha(1950)$	6(1950)	Flux (Jy)				$L(L_\odot)$	Association
			$12\mu m$	$25\mu m$	$60\mu m$	$100\mu m$		
1 06314+0421	0631 28.1	042126	0.7	1.6	105	323.6	73'7	Globule 7
2 06314+0427	063126.6	04271'7	6.1	6.5	129.3	323.6	924	CO peak (IRS)
3 0631 8+0420	063153.6	042013	1.5	3.8	36.6	995.2	136S	
4 06319+0415	063159.0	041509	7s.4	375.8	95s.s	995.2	7622	AFGL 961
5 06322+0427	0632 16.5	042'740	0.4	0.7	10.2	73.9	131	Globule 1
6 06327+0423	063247.0	042313	0.5	0.S	S.2	62.7	114	Globule 3
7 X0632+043	063231.6	042346				299		Globule 3

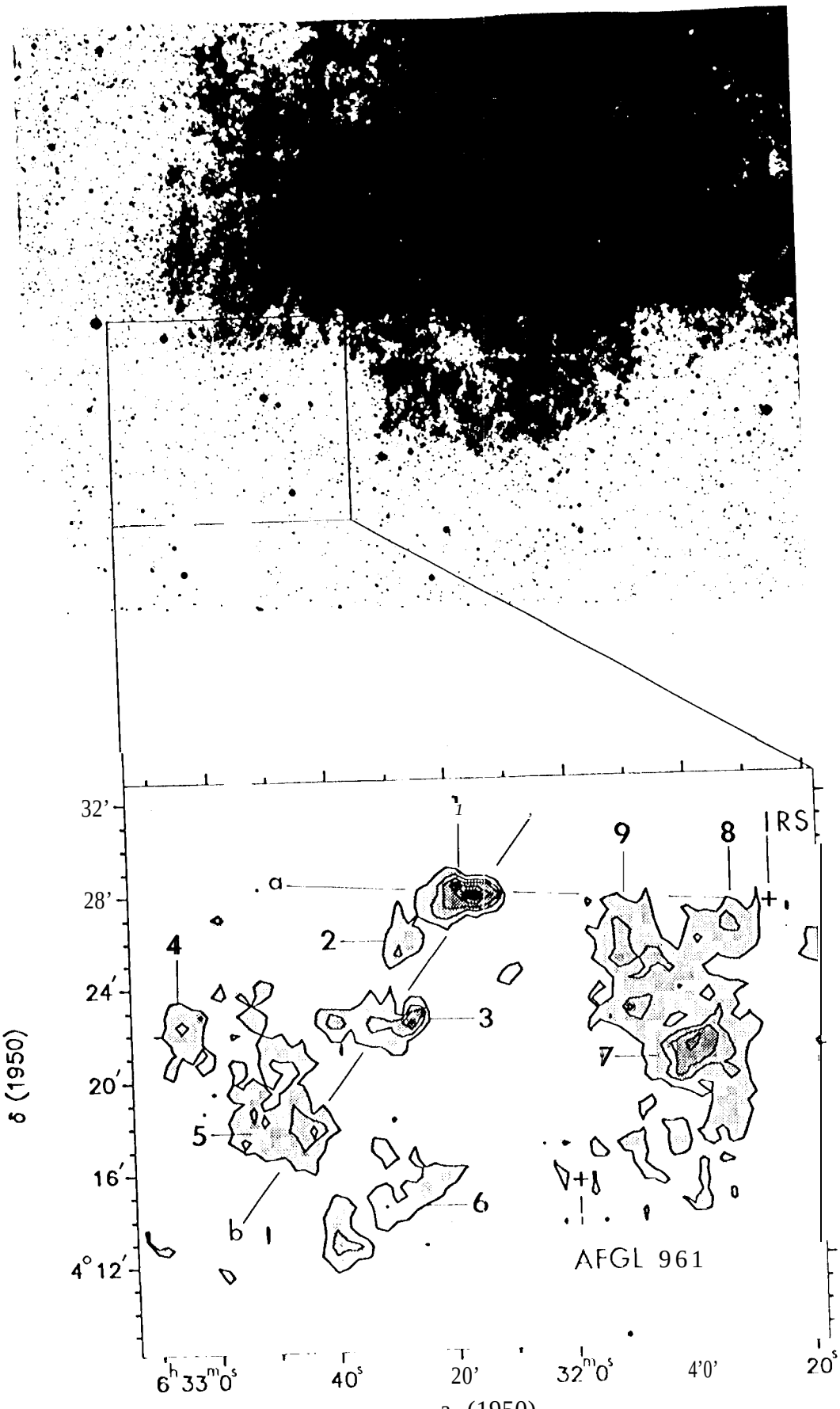
32'
28'
24'
20'
16'
4° 12'
δ (1950)
1
9
8
IRS
a
2
4
3
7
5
6
b
AFGL 961
6h 33m 0s
40s
20'
32m 0s
4'0'
20s
a (1950)

Fig. 2a

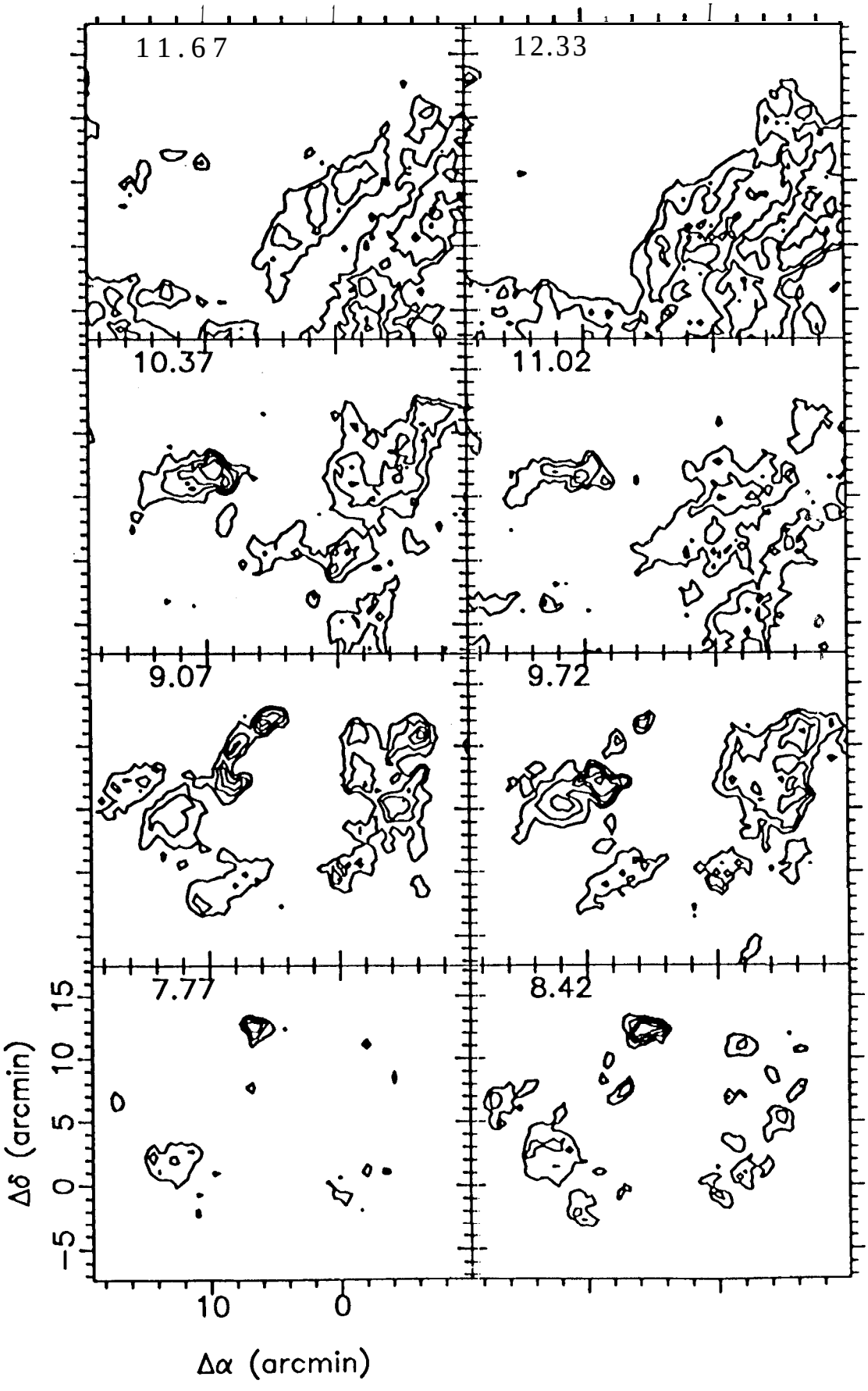
11.67
12.33
10.37
11.02
9.07
9.72
7.77
8.42
15
10
5
0
−5
Δδ (arcmin)
10
0
Δα (arcmin)

Fig. 2b

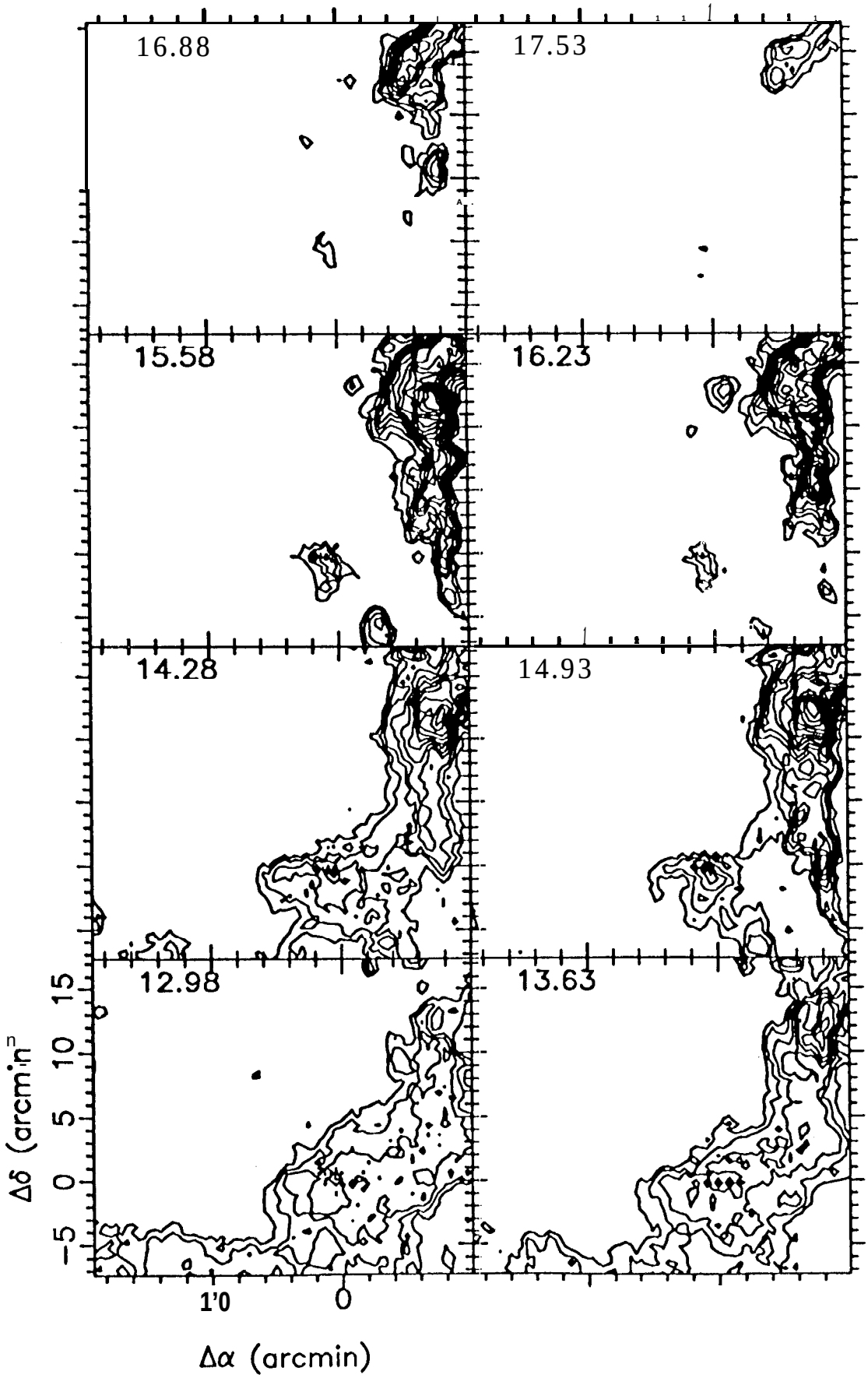
16.88
17.53
15.58
16.23
14.28
14.93
12.98
13.63
Δδ (arcmin)
15
10
5
0
−5
1'0
0
Δα (arcmin)

Fig. 3a

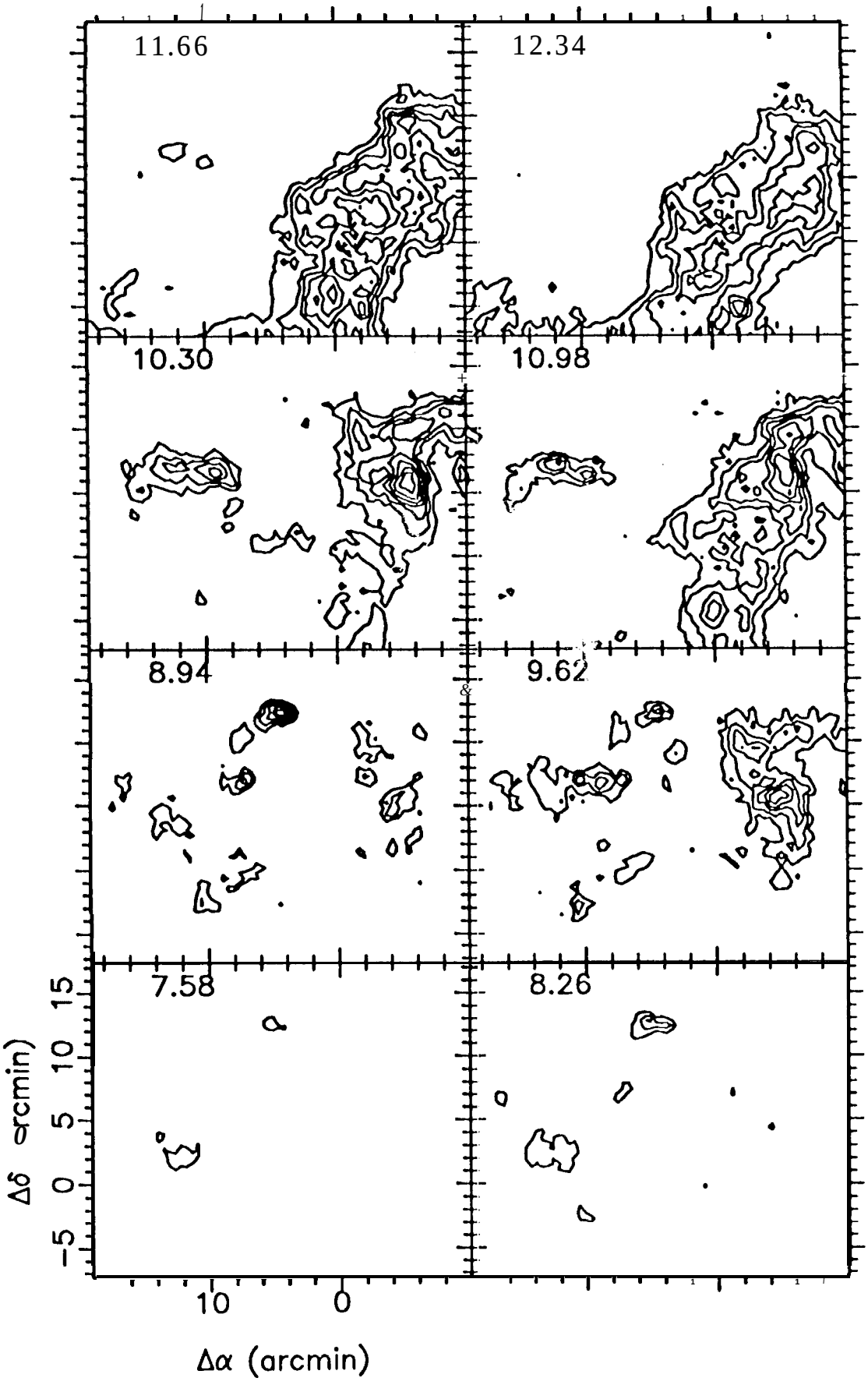
11.66
12.34
10.30
10.98
8.94
9.62
7.58
8.26
15
10
5
0
−5
Δδ (arcmin)
10
0
Δα (arcmin)

Fig. 3b

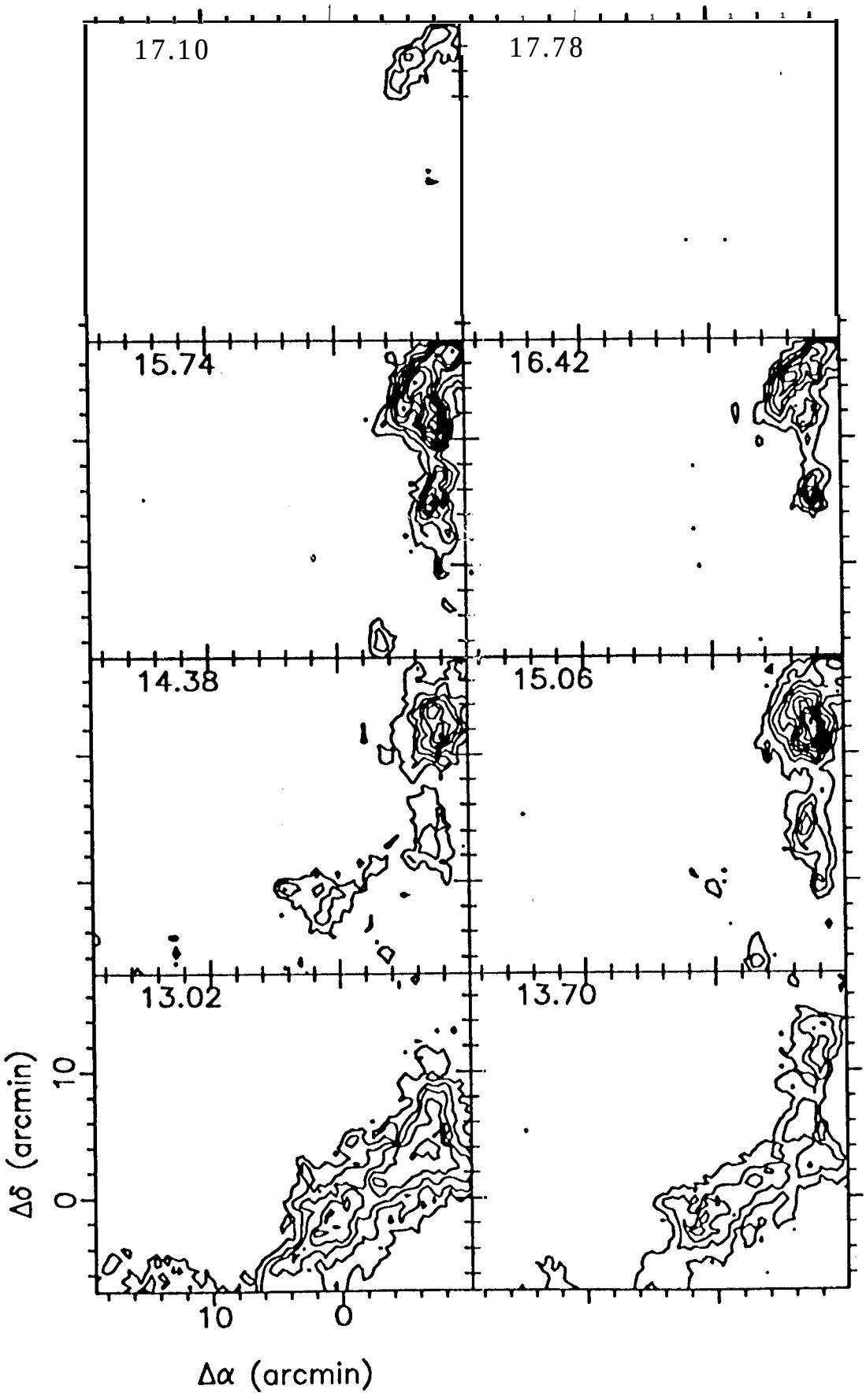
17.10
17.78
15.74
16.42
14.38
15.06
13.02
13.70
10
0
Δδ (arcmin)
10
0
Δα (arcmin)

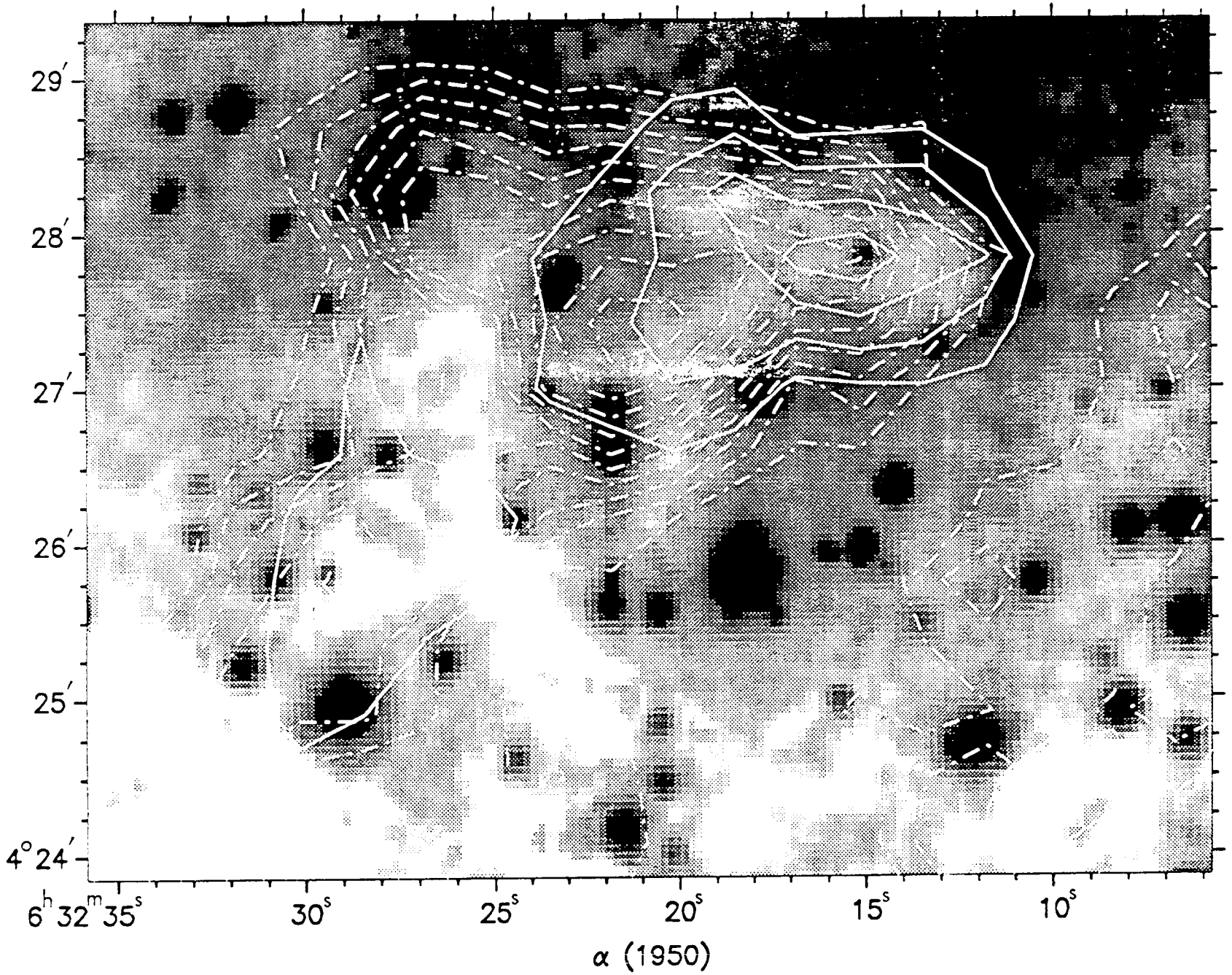

Fig. 4

Fig. 5

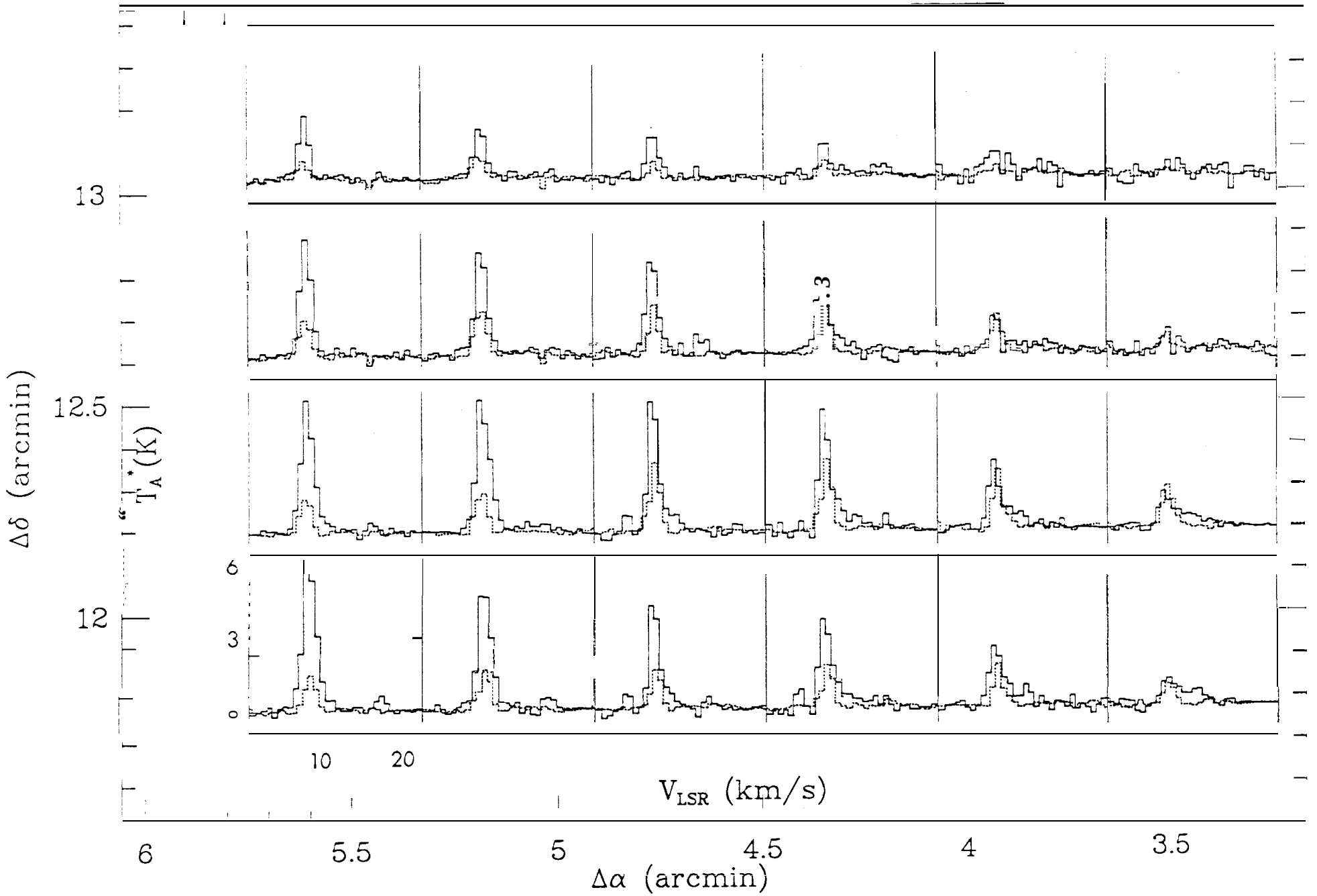

Fig 6

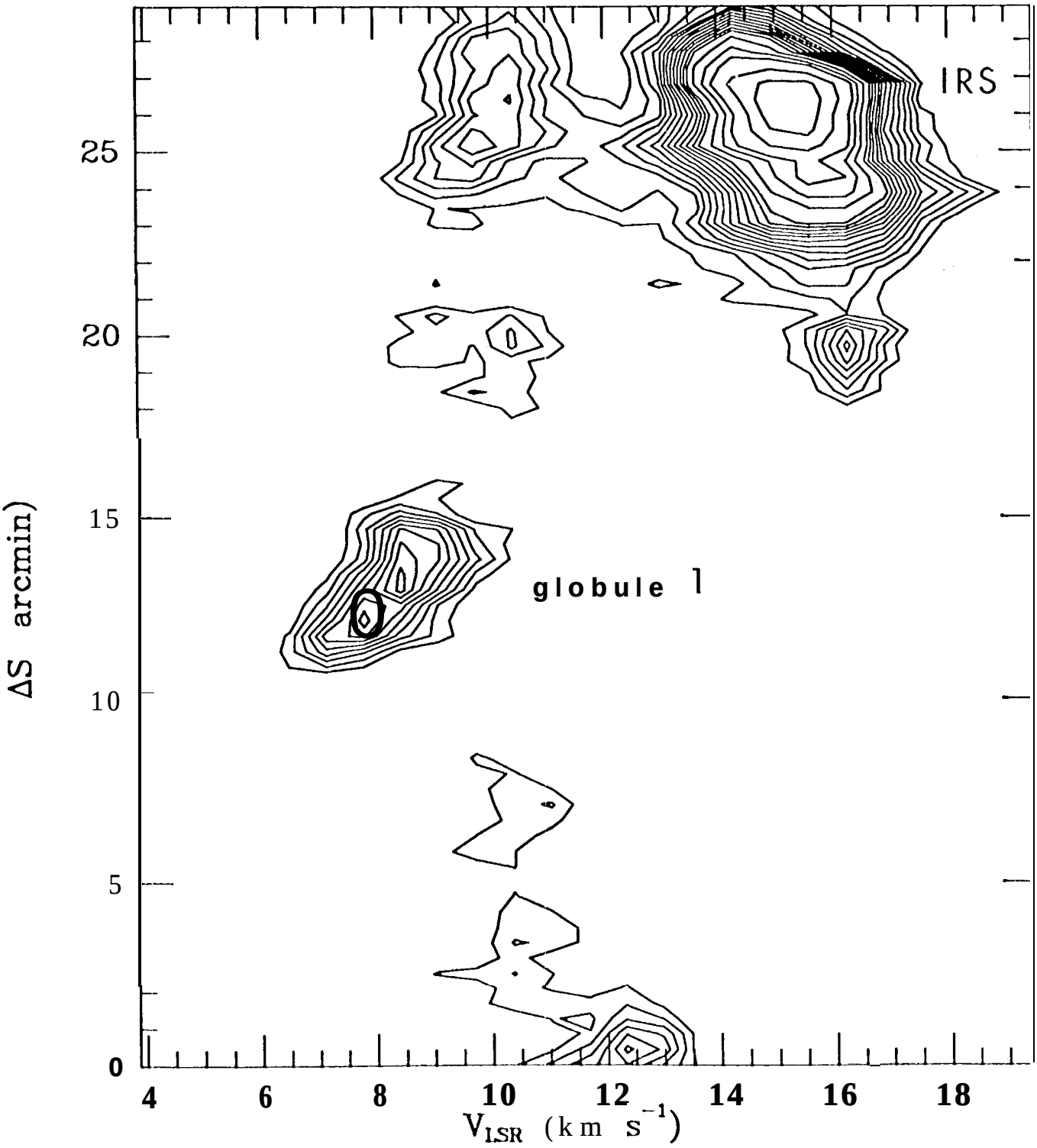
IRS
globule 1
25
20
15
10
5
0
ΔS arcmin)
4
6
8
10
12
14
16
18
V_{LSR} (km s^{-1})

Fig. 7

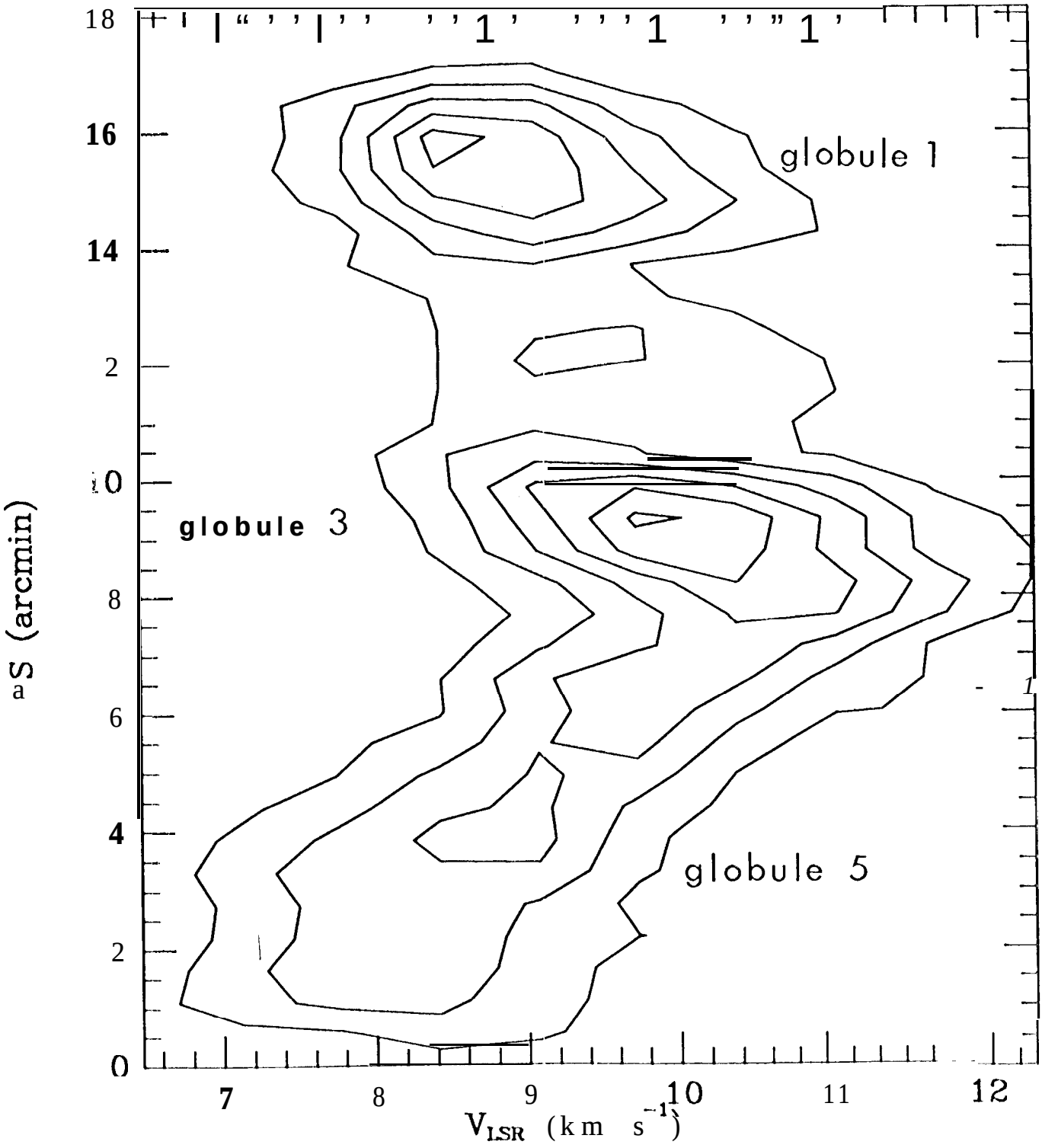
globule 1
globule 3
globule 5
18
16
14
2
10
8
6
4
2
0
7
8
9
10
11
12
ΔS (arcmin)
V_{LSR} (km s^{-1})

Fig. 8

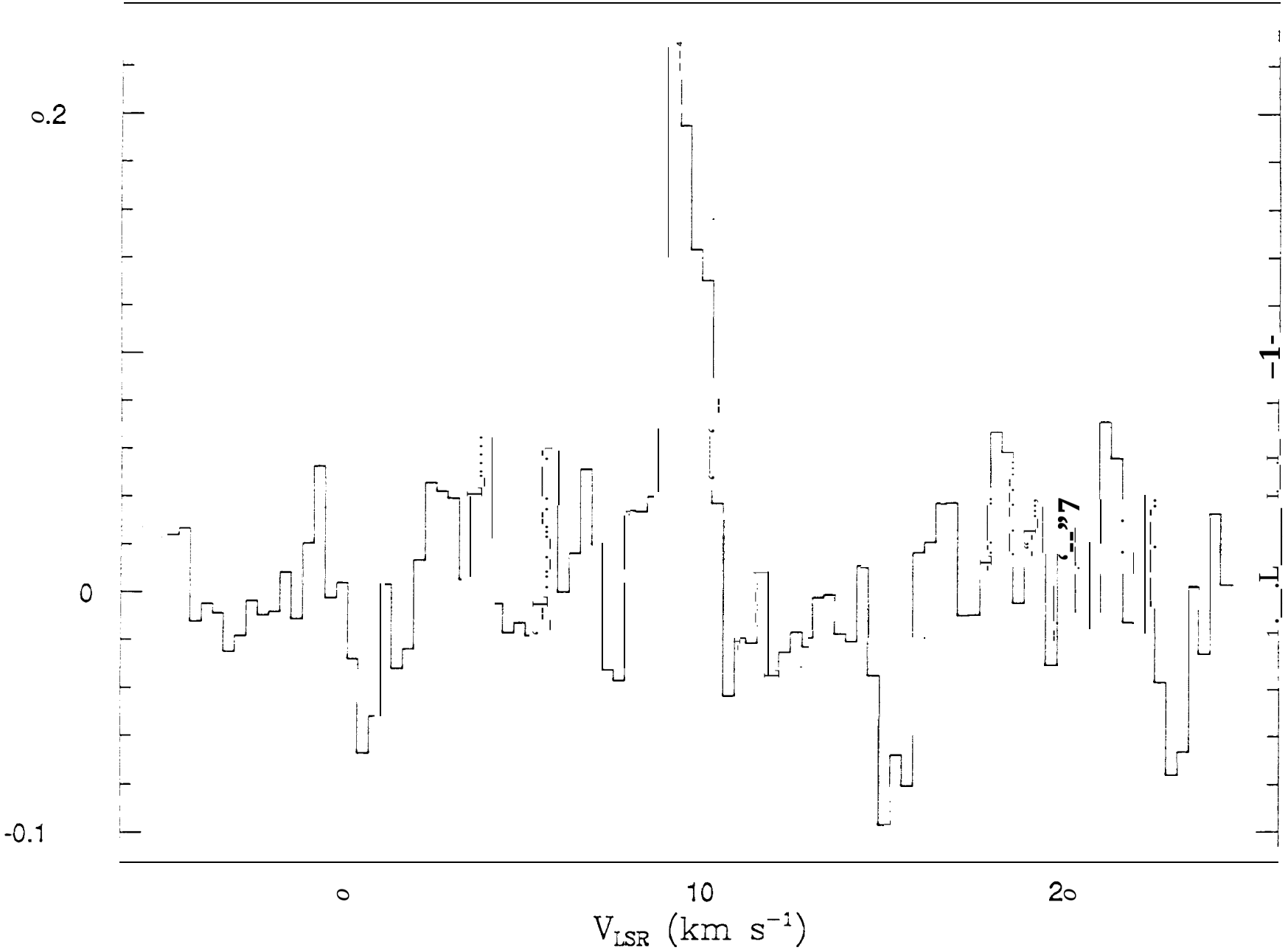

Fig. 9

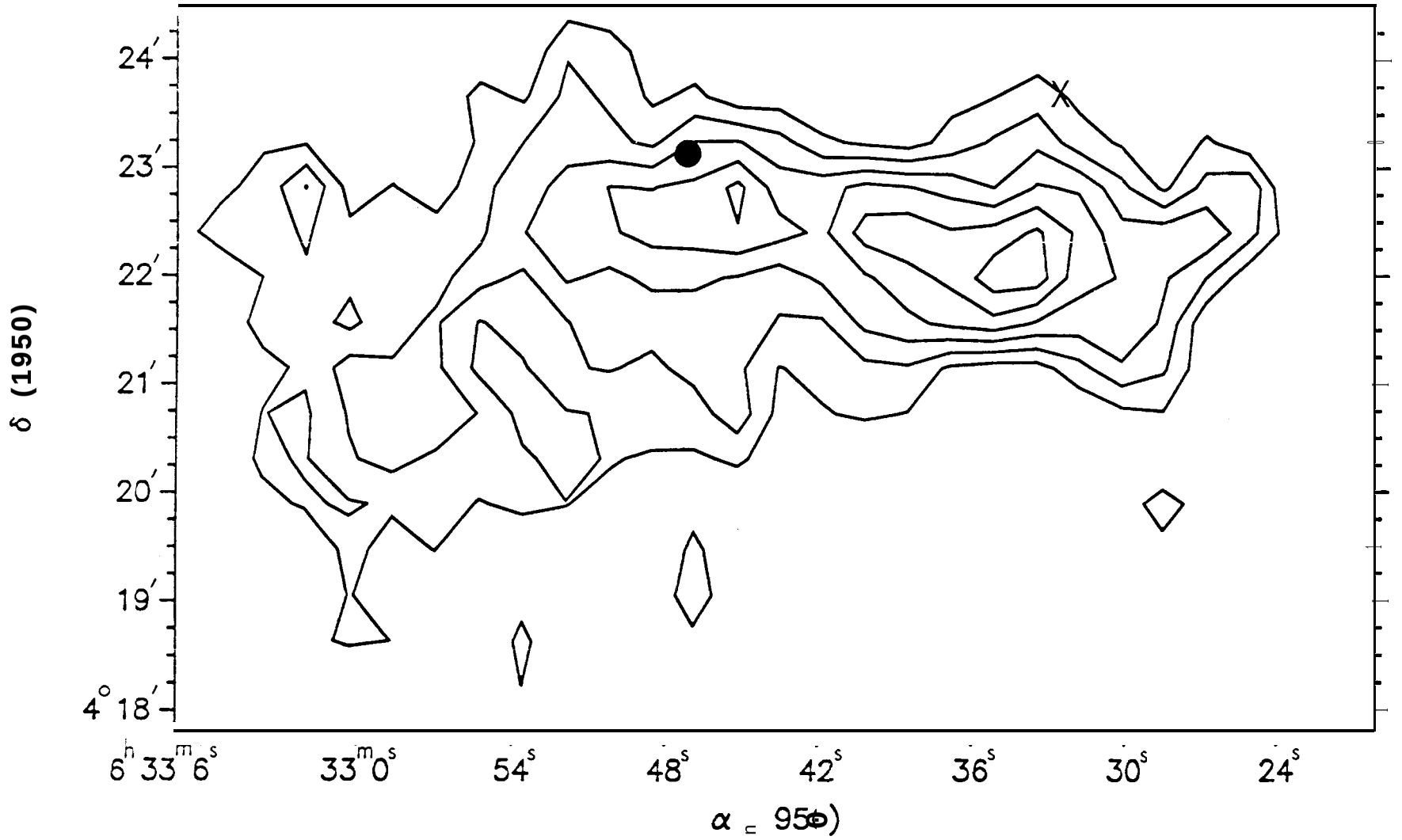
24′
23′
22′
21′
20′
19′
4° 18′
δ (1950)
6h 33m 6s
33m 0s
54s
48s
42s
36s
30s
24s
α (1950)

Fig. 10